$Li_{0.33}La_{0.557}TiO_3$@$BaTiO_3$ core-shell fiber as fillers to promote the dissociation and migration of lithium-ions in the solid polymer electrolytes

Zhihao Ding[1#], Jianjun Song[1#], Lei Zhang[1], Peng Guo[1], Chaoyan Zhang[1], Chuan Shi[1*]

[1] College of Physics, Qingdao University, Qingdao 266071, China. E-mail:

chuanshi@qdu.edu.cn

#Zhihao Ding and Jianjun Song contributed equally to this work.

Calculation Method：

First-principles calculations are performed by vienna ab initio simulation package (VASP).[1, 2] The generalized gradient approximation (GGA) of Perdew-Burke-Ernzerhof (PBE) is used to describe the exchange-correlation functional.[3] To accurately describe the dispersion interactions in our simulations, the DFT-D3 method was employed.[4]

Li@$BaTiO_3$: The cut-off energy for the plane wave basis is set to 500 eV and a 4×4×1 Monkhorst-pack mesh is employed. All atoms were fully relaxed (atomic position) up to 10^{-4}eV/Å force minimization and max force of 0.05 eV/ Å. The DFT+U method was used to calculate the electronic properties.[5]

Li@LLTO: The cut-off energy for the plane wave basis is set to 500 eV and a 3×2×1 Monkhorst-pack mesh is employed. All atoms were fully relaxed (atomic position) up to 10^{-4} eV/Å force minimization and max force of 0.05 eV/ Å. The DFT+U method was used to calculate the electronic properties.[5]

Experimental Section

Preparation of LLTO@BTO nanowires:

Firstly, we prepared electrospinning precursor solutions of LLTO and BTO:

(1) LLTO precursor solution: Lithium nitrate ($LiNO_3$, Aladdin, 99.9%), Lanthanum nitrate hexahydrate ($La(NO_3)_3·6H_2O$, Aladdin, 99.99%) and Polyvinylpyrrolidone

(PVP, Aladdin, MW=1300000) were dissolved in N, N-Dimethylformamide (DMF, Hushi, AR) and Acetic acid (AC, Macklin, ≥99.9%) solvent at a certain mass ratio and stirred for 12 hours. Then Titanium butoxide ($C_{16}H_{36}O_4Ti$, Aladdin, 98%) was added and stirred well to obtain a uniformly mixed solution.

(2) $BaTiO_3$ precursor solution: Barium acetate ($(CH_3COO)_2Ba$, Hushi, AR) and PVP were dissolved in Acetic acid, Absolute ethanol (AE, Hushi, AR) and deionized water solvent at a certain mass ratio, stirred for 12 hours, then Titanium butoxide was added and stirred for 1 hour to obtain a uniformly mixed solution.

Secondly, We prepare LLTO@BTO and LLTO nanowires by electrospinning:

The above two precursor solutions were coaxial electrospinning. By using a coaxial electrospinning needle, the fiber film was spun at a voltage of 15 kV, a propulsion rate of 10 ul min^{-1}, a receiving distance of 10 cm, and a drum speed of 200 r min^{-1} were used to obtain a fiber film and dry. The obtained fiber membrane was sintered at 900 °C for 1 hour, the heating rate was 3 °C min^{-1}, and coaxial BTO@LLTO nanowires were obtained. In addition, a single needle was used for the preparation of LLTO nanowires, and other conditions were consistent.

Preparation of Composite Solid Electrolytes:

BTO@LLTO coaxial nanofibers and LLTO nanofibers are ground into staple fibers as inorganic fillers. BTO@LLTO or LLTO (5%, 10%, 15%, 20% by mass), Polyethylene oxide (PEO, Macklin, MW=1000000) and Lithium bis-trifluoromethane sulfonamide (LiTFSI, Aladdin, 99.99 %) were dissolved in Acetonitrile solvent, stirred well, and then coated on a PTFE plate to dry to form an electrolyte film. They were called PEO-LLTO@BTO and PEO-LLTO, separately.

Preparation of cathode:

$LiFePO_4$(LFP), Super-P, PVDF and SCN were mixed in a weight ratio of 7:1:1:1 to prepare the cathode. First of all, we needed to grind $LiFePO_4$ and Super-P evenly, add PVDF solution and SCN solution, and stir to obtain a uniform cathode slurry. Subsequently, the uniform slurry was coated on the foil and dried in a vacuum oven at 60 ℃. Finally, the dried pole piece was stored for subsequent battery installation.

Characterization of the electrolytes:

The crystal structures of LLTO@BTO and LLTO were observed by X-ray diffraction (XRD, Bruker D2 Phaser). The morphology, structure, and element mapping of the materials were characterized by field-emission scanning electron microscopy (FE - SU8100, Hitachi, Japan), and the diameter distributions before and after calcination were statistically analyzed.

The structures of LLTO and LLTO@BTO were observed by transmission electron microscopy (TEM, JEM - 2100F, JEOL). Differential scanning calorimetry (DSC, SDT - 650, TA Instruments, Milford, USA) and thermogravimetry (TG) were used to study the melting temperatures and thermal stabilities of pure PEO, PEO - LLTO and PEO - LLTO@BTO.

X-ray photoelectron spectroscopy (XPS, Thermo Fisher Scientific, USA) analysis confirmed the states of elements.

Electrochemical Testing:

We used the Electrochemical workstation (CHI760E) and Neware batteries tester (Neware company, China) to test the Electrochemical performance. The different batteries were assembled in an Ar-filled glove box（the water content < 0.1 ppm, the oxygen content < 0.1 ppm）. Assemble stainless steel gasket symmetric cells to perform AC impedance measurement under the conditions of 30-60 °C, 100 kHz-1 Hz, and an amplitude of 10 mV. Calculate their ionic conductivities at different temperatures by the formula $\sigma = \frac{L}{RS}$ (where σ is the ionic conductivity, L is the thickness of the solid-state electrolyte membrane, R is the resistance, and S is the contact area), and calculate the activation energy by the Arrhenius formula. Assemble gasket|SPE|Li cells. Each cell was subjected to an electrochemical stability test of the solid-state electrolyte membrane by linear sweep voltammetry (LSV) at a scan rate of 0.1 mV s^{-1} in the range of 0-6 V. Through the polarization test of Li-symmetric cells at different current densities, the dynamic interface stability between SPEs and Li metal at the working temperature was studied. Use the above-obtained cathode sheets to assemble LFP/Li cells and pouch cells and then test them to evaluate their cycling performance and practical applications. The redox stability of different composite solid

electrolytes and the reversibility of LFP/Li cells were determined by cyclic voltammetry (CV) at a scanning rate of 0.1 mV s^{-1} in the voltage range of 3 V-4 V.

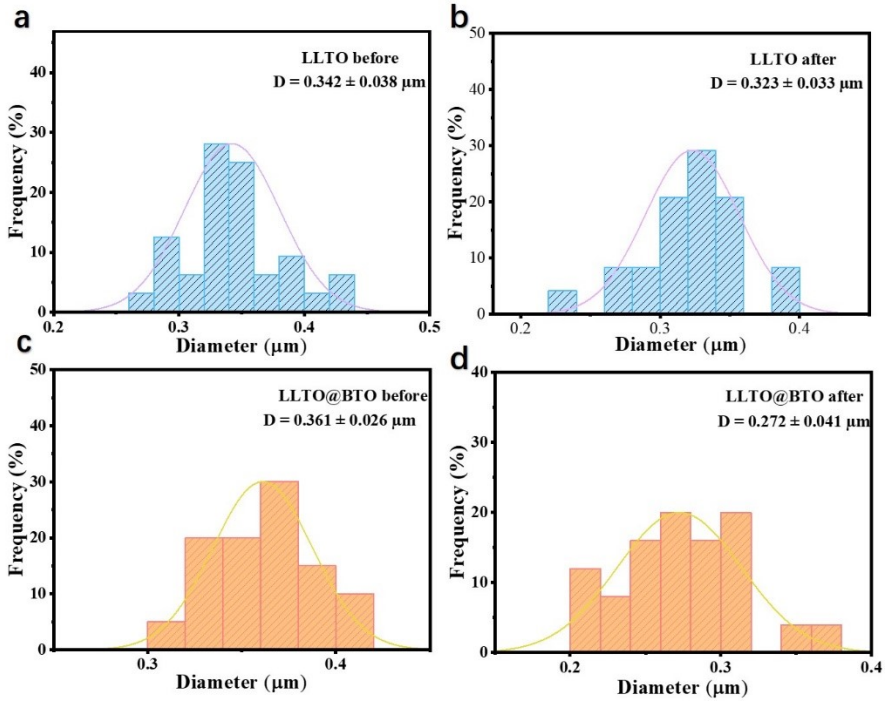

Figure S1 Diameter distribution of LLTO nanofibers before (a) and after calcination (b); Diameter distribution of LLTO@BTO nanofibers before (c) and after calcination (d).

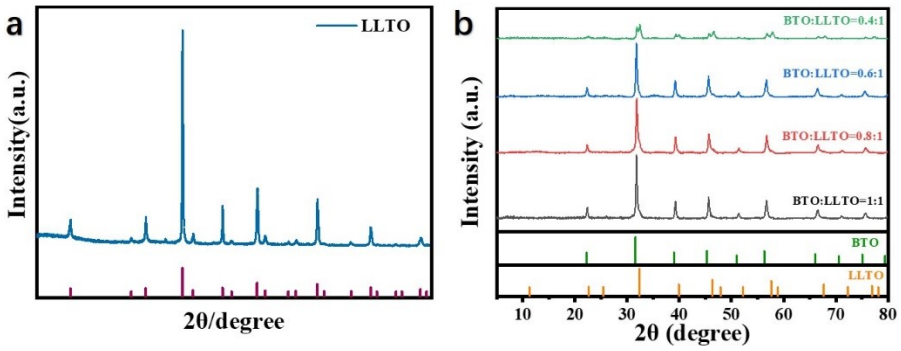

Figure S2 (a) XRD profile of LLTO. (b)XRD spectra of different BTO: LLTO (puta-to-core ratio) ratios.

The LLTO is encapsulated by BTO and the LLTO@BTO only exhibits the the crystal peaks of pure BTO with a BTO: LLTO ratio of 1:1. The crystal peaks of LLTO of LLTO: BTO gradually appear with decreasing the BTO: LLTO ratio from 1:1 to 0.4:1.

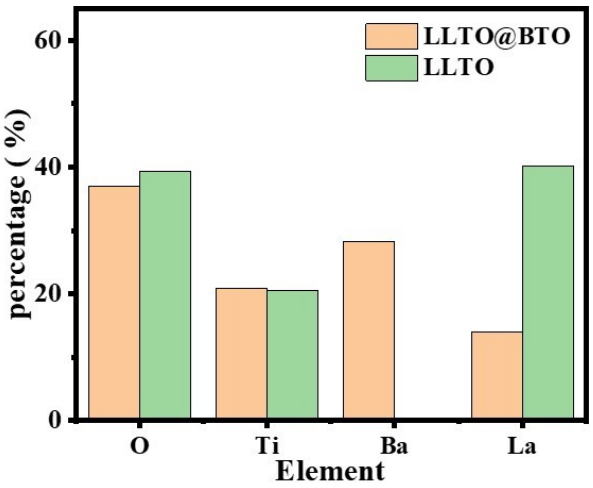

Figure S3 EDS element content of LLTO and LLTO@BTO.

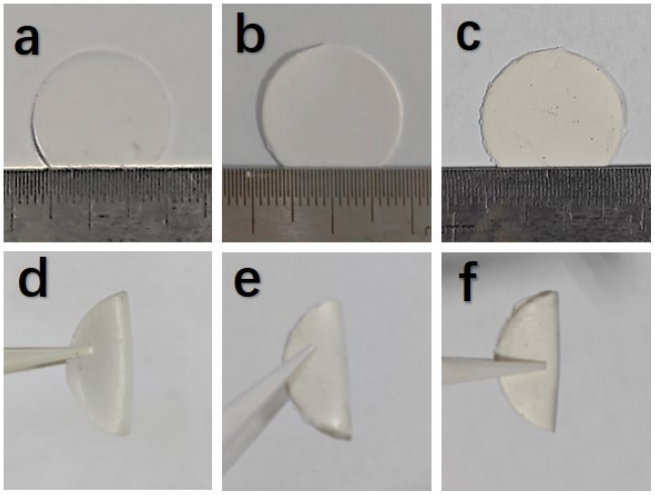

Figure S4 Digital images of different solid-state electrolytes: (a) (d) is PEO solid-state electrolyte, (b) (e) is PEO-LLTO solid-state electrolyte, and (c) (f) is PEO-LLTO@BTO solid-state electrolyte.

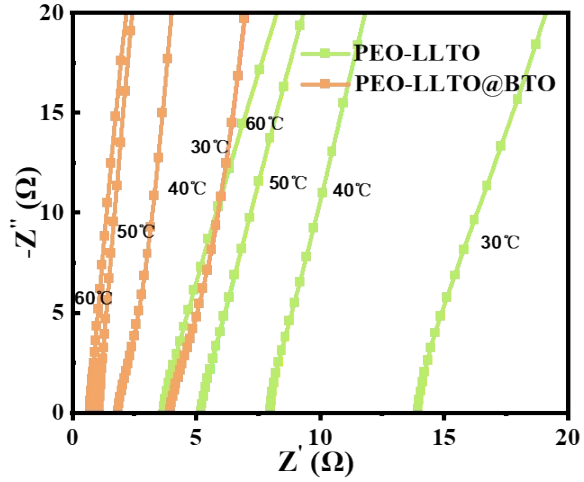

Figure S5 Impedance plot of PEO-LLTO and PEO-LLTO@BTO as a function of temperature.

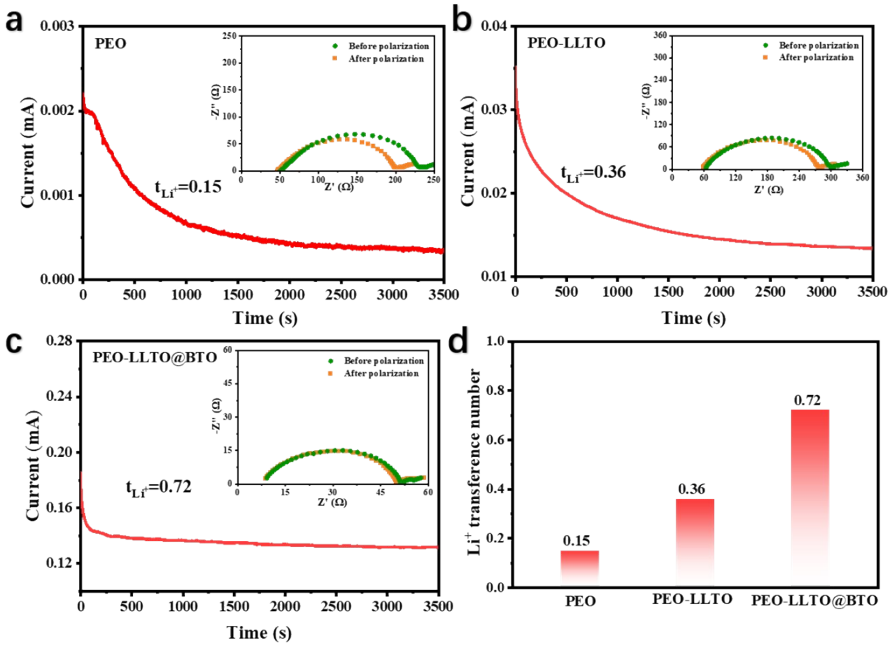

Figure S6 Polarization curves and initial and steady-state impedance plots (insets) for (a) PEO, (b) PEO-LLTO, and (c) PEO-LLTO@BTO. Calculation of the number of lithium transfers in a PEO-based electrolyte(d).

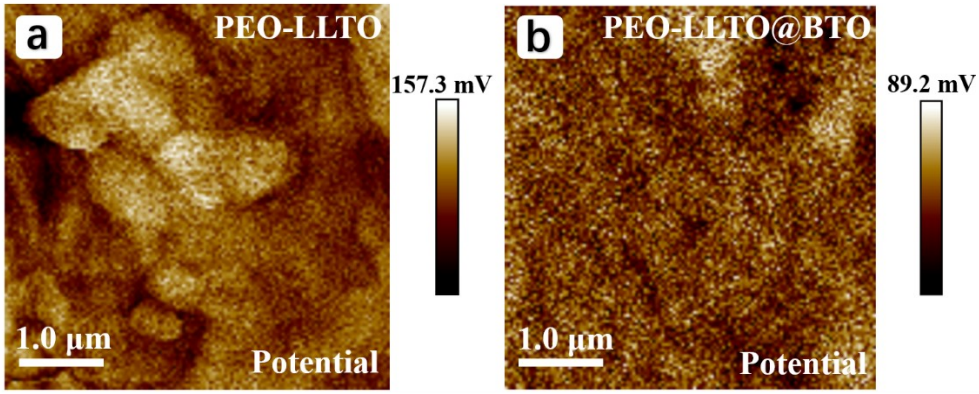

Figure S7 Kelvin probe force microscopy interface potential images of PEO-LLTO (a) and PEO-LLTO@BTO (b) electrolytes.

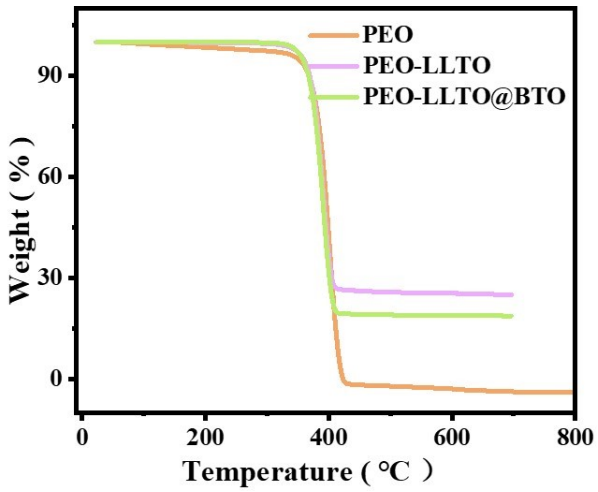

Figure S8 TG curves of PEO, PEO-LLTO, and PEO-LLTO@BTO

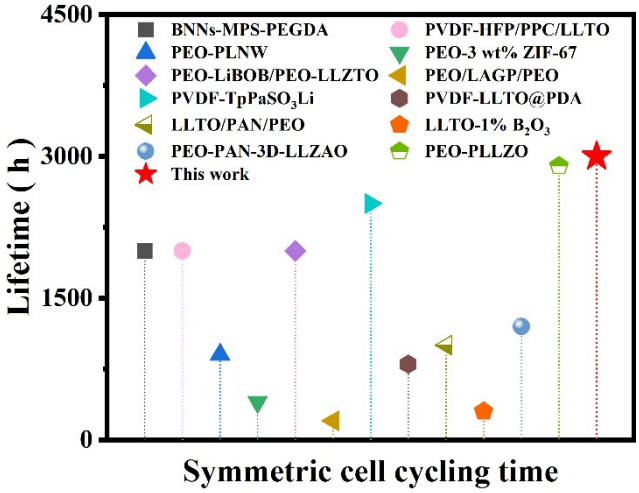

Figure S9 Cycling time with recently reported articles.[6-17]

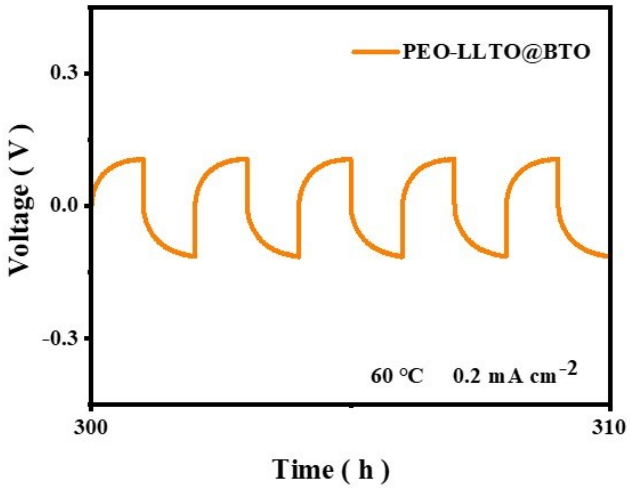

Figure S10 Enlarged picture of the cycling performance of a Li symmetrical cell of PEO-LLTO@BTO at 0.2 mA cm^{-2} and 60 °C.

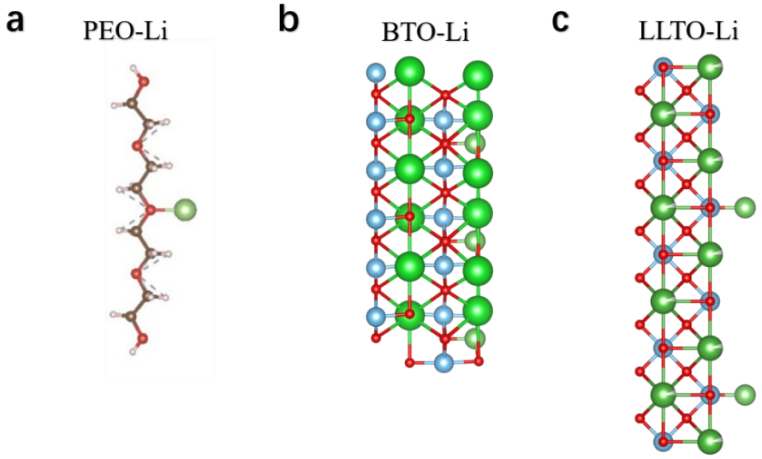

Figure S11 The Li affinity comparison of (a) PEO molecules、(b) $BaTiO_3$ and (c) LLTO toward Li atom.

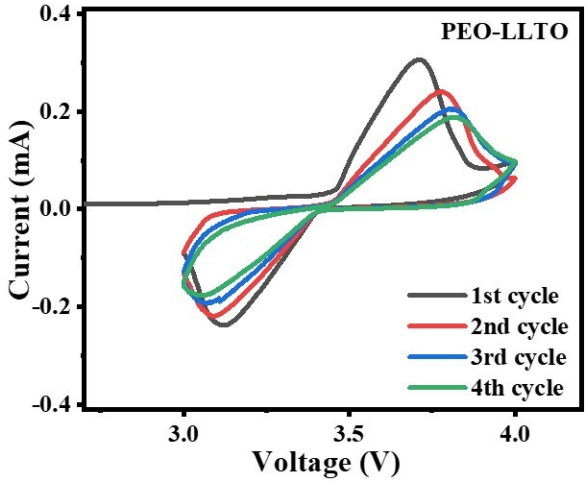

Figure S12 The CV curves of cells with PEO-LLTO.

Table S1. Recently studied the ionic conductivity and electrochemical stability window performance of some solid-state electrolytes.

Polymer	**Fillers**	**δ (S cm^{-1})**	**EW(V)**	**Reference**
PVDF	Y-LZNO	2.34 x 10^{-4} (RT)	4.82	[18]
PVDF	LTO	2.87 x 10^{-4} (35 ℃)	5.0	[19]
PVDF-HFP	LLTO	1.21 x 10^{-4} (25 ℃)	4.7	[20]
PEO+PEG	LATP	1.31 x 10^{-4} (30 ℃)	5.5	[21]
PEO	SiO_2-Aerogel	0.6 x 10^{-3} (30 ℃)	4.4	[22]
PEO	LLZTO@PDA	1.15 x 10^{-4} (30 ℃）	4.8	[23]
PEO	SN	3.0 x 10^{-5} (20 ℃)	4.0	[24]
PEO	SN-LLZTO	6.74 x 10^{-4} (RT)	4.7	[25]
PPO	LLZO	4.59 x 10^{-4} (RT)	5.3	[26]
PPO	LAGP	3.46 x 10^{-4} (RT)	4.78	[27]
PEGDA	LLZTO+SN	3.1 x 10^{-4} (RT)	4.7	[28]
PEO	LLTO@BTO	1.44 x 10^{-3} (30 ℃)	5.0	This work

Reference：

1. G. Kresse and J. Furthmüller, *Computational Materials Science*, 1996, **6**, 15-50.
2. G. Kresse and D. Joubert, *Physical Review B*, 1999, **59**, 1758-1775.
3. J. P. Perdew, K. Burke and M. Ernzerhof, *Physical Review Letters*, 1996, **77**, 3865-3868.
4. S. Grimme, J. Antony, S. Ehrlich and H. Krieg, *The Journal of Chemical Physics*, 2010, **132**, 154104.
5. V. I. Anisimov, J. Zaanen and O. K. Andersen, *Physical Review B*, 1991, **44**, 943-954.
6. H. An, Q. Liu, J. An, S. Liang, X. Wang, Z. Xu, Y. Tong, H. Huo, N. Sun, Y. Wang, Y. Shi and J. Wang, *Energy Storage Materials*, 2021, **43**, 358-364.
7. F. Fei, H. Zhang, J. Deng, H. Xu, J. Xie, H. S. H. Mohamed, A. E. Abdelmaoula, L. Mai and L. Xu, *ACS Applied Materials & Interfaces*, 2023, **15**, 30170-30178.
8. H.-L. Guo, H. Sun, Z.-L. Jiang, J.-Y. Hu, C.-S. Luo, M.-Y. Gao, J.-Y. Cheng, W.-K. Shi, H.-J. Zhou and S.-G. Sun, *ACS Applied Materials & Interfaces*, 2019, **11**, 46783-46791.
9. M. Jia, Z. Bi, C. Shi, N. Zhao and X. Guo, *ACS Applied Materials & Interfaces*, 2020, **12**, 46231-46238.
10. Z. Wu, Z. Wu, Z. Wang, Y. Peng, Z. Li, Z. Huang, W. Mei, D. Liu, M. Li, W. Zhou, F. Gao, Z. Cheng and G. Luo, *Corrosion Science*, 2023, **224**, 111473.
11. T.-Q. Yang, C. Wang, W.-K. Zhang, Y. Xia, Y.-P. Gan, H. Huang, X.-P. He and J. Zhang, *Rare Metals*, 2022, **41**, 1870-1879.
12. Z. Yang, H. Yuan, C. Zhou, Y. Wu, W. Tang, S. Sang and H. Liu, *Chemical Engineering Journal*, 2020, **392**, 123650.
13. C. Zhang, Z. Jiang, P. Guo, J. Song and C. Shi, *Chemical Engineering Journal*, 2025, **503**, 158146.
14. Q. Zhang, R. Yang, C. Li, M. Luo, B. Wang, W. Yu, Y. Yan, Y. Zou, L. Zhong and Y. Xu, *Ceramics International*, 2025, DOI: https://doi.org/10.1016/j.ceramint.2025.01.113.
15. Y. Zhang, L. Zhang, P. Guo, C. Zhang, X. Ren, Z. Jiang, J. Song and C. Shi, *Nano Research*, 2024, **17**, 2663-2670.
16. E. Zhao, Y. Guo, Y. Liu, S. Liu and G. Xu, *Applied Surface Science*, 2022, **573**, 151489.
17. L. Zhu, H. Xie, W. Zheng and K. Zhang, *Electrochimica Acta*, 2022, **435**, 141384.
18. J. Chen, H. Zhang, H. Chen, E. Xia, Y. Wu and Z. Li, *Journal of Power Sources*, 2022, **548**, 232109.
19. Q. Zhou, X. Yang, X. Xiong, Q. Zhang, B. Peng, Y. Chen, Z. Wang, L. Fu and Y. Wu, *Advanced Energy Materials*, 2022, **12**, 2201991.
20. J. Li, L. Zhu, J. Zhang, M. Jing, S. Yao, X. Shen, S. Li and F. Tu, *International Journal of Energy Research*, 2021, **45**, 7663-7674.
21. Y.-H. Song, Y.-C. Chen, E.-C. Lin, T. Y. Liang, C. Y. Wu, A.-Y. Wang, H.-Y.

Chen and J. M. Wu, *Journal of Materials Chemistry A*, 2024, **12**, 26809-26819.
22. D. Lin, P. Y. Yuen, Y. Liu, W. Liu, N. Liu, R. H. Dauskardt and Y. Cui, *Advanced Materials*, 2018, **30**, 1802661.
23. Z. Huang, W. Pang, P. Liang, Z. Jin, N. Grundish, Y. Li and C.-A. Wang, *Journal of Materials Chemistry A*, 2019, **7**, 16425-16436.
24. V. van Laack, F. Langer, A. Hartwig and K. Koschek, *ACS Omega*, 2023, **8**, 9058-9066.
25. X. Zhang, C. Fu, S. Cheng, C. Zhang, L. Zhang, M. Jiang, J. Wang, Y. Ma, P. Zuo, C. Du, Y. Gao, G. Yin and H. Huo, *Energy Storage Materials*, 2023, **56**, 121-131.
26. J. Li, L. Zhong, J.-x. Li, H.-f. Wu, W.-w. Shao, P.-q. Wang, M.-q. Liu, G. Zhang and M.-x. Jing, *Colloids and Surfaces A: Physicochemical and Engineering Aspects*, 2023, **671**, 131704.
27. Z.-h. Huang, J. Li, L.-x. Li, H.-m. Xu, C. Han, M.-q. Liu, J. Xiang, X.-q. Shen and M.-x. Jing, *Ceramics International*, 2022, **48**, 25949-25957.
28. X. Yu, Y. Liu, J. B. Goodenough and A. Manthiram, *ACS Applied Materials & Interfaces*, 2021, **13**, 30703-30711.